Astronomy & Astrophysics manuscript no. main
October 16, 2024

Analysis of the Blazhko effect for field RR Lyrae stars

using LINEAR and ZTF light curves

Ema Donev[1] and Željko Ivezić[2]

[1] XV. Gymnasium (MIOC), Zagreb, Croatia, e-mail: emadonev@icloud.com
[2] Department of Astronomy, University of Washington, Box 351580, Seattle, WA 98195, USA, e-mail: ivezic@uw.edu

October 2024

ABSTRACT

We analyzed the incidence and properties of stars that show evidence for amplitude, period, and phase modulation (the so-called Blazhko Effect) in a sample of ∼3,000 field RR Lyrae stars with LINEAR and ZTF light curve data. A preliminary subsample of about ∼240 stars was selected using various light curve statistics, and then ∼140 stars were confirmed visually as displaying the Blazhko effect. Although close to 8,000 Blazhko stars were discovered in the Galactic bulge and LMC/SMC by the OGLE-III survey, only about 200 stars have been reported in all field RR Lyrae stars studies to date.

Key words. Variable stars — RR Lyrae stars — Blazhko Effect

1. Introduction

RR Lyrae stars are pulsating variable stars with periods in the range of 3–30 hours and large amplitudes that increase towards blue optical bands (e.g., in the SDSS g band from 0.2 mag to 1.5 mag; Sesar et al. 2010). For comprehensive reviews of RR Lyrae stars, we refer the reader to Smith (1995) and Catelan (2009).

They often exhibit amplitude, period, and phase modulation, or the so-called Blazhko effect (hereafter, "Blazhko stars"). For examples of well-sampled observed light curves showing the Blazhko effect, see, e.g., Kepler data shown in Figures 1 and 2 from Benkő et al. (2010). The effect has been known for a long time (Blažko 1907), but its detailed observational properties and theoretical explanation of its causes remain elusive Kovács (2009).

References to various proposed models for the mysterious Blazhko effect and main reasons why they fail to explain observations are summarized in Kovacs (2016).

A part of the reason for the incomplete observational description of the Blazhko effect is difficulties in discovering a large number of Blazhko stars due to temporal baselines that are too short and insufficient number of observations per object (Kovacs 2016; Hernitschek & Stassun 2022). With the advent of modern sky surveys, several studies reported large increases in the number of known Blazhko stars, starting with a sample of about 700 Blazhko stars discovered by the MACHO survey towards LMC (Alcock et al. 2003) and about 500 Blazhko stars discovered by the OGLE-II survey towards the Galactic bulge (Mizerski 2003). Most recently, about 4,000 Blazhko stars were discovered in the Large and Small Magellanic Clouds (Soszyński et al. 2009, 2010), and an additional ∼3,500 stars were discovered in the Galactic bulge (Soszyński et al. 2011), both by the OGLE-III survey. Nevertheless, discovering the Blazhko effect in field RR Lyrae stars that are spread over the entire sky remains a much harder problem: only about 200 Blazhko stars in total from all the studies of field RR Lyrae stars have been reported so far (see Table 1 in Kovacs 2016).

Here, we report the results of a search for the Blazhko effect in a sample of ∼3,000 field RR Lyrae stars with LINEAR and ZTF light curve data. A preliminary subsample of about ∼240 stars was selected using various light curve statistics, and then ∼140 stars were confirmed visually as displaying the Blazhko effect. This new sample greatly increases the number of known field RR Lyrae stars that exhibit the Blazhko effect. In §2 we describe our datasets and analysis methodology, and in §3 we present our analysis results. Our main results are summarized and discussed in §4.

2. Data Description and Analysis Methodology

Our chosen surveys for this project were the LINEAR asteroid survey and, subsequently, the ZTF survey, from which we selected the corresponding LINEAR stars. The ZTF survey monitored the sky ∼10 years after LINEAR, providing a unique opportunity for analysis. In this work, we used the programming language Python. The entirety of the code can be found on GitHub[1].

2.1. LINEAR Dataset

The properties of the LINEAR asteroid survey and its photometric re-calibration based on SDSS data are discussed in Sesar et al. (2011). Briefly, the LINEAR survey covered about 10,000 deg^2 of the northern sky in white light (no filters were used, see Figure 1 in Sesar et al. 2011), with photometric errors ranging from ∼0.03 mag at an equivalent SDSS magnitude of $r = 15$ to 0.20 mag at $r \sim 18$. Light curves used in this work include, on average, 270 data points collected better between December 2002 and March 2008.

A sample of 7,010 periodic variable stars with $r < 17$ discovered in LINEAR data was robustly classified by Palaversa

[1] https://github.com/emadonev/var_stars

et al. (2013), including about ~3,000 field RR Lyrae stars detected to distances of about 30 kpc (Sesar et al. 2013) of both ab and c type. The sample used in this work contains 2196 ab-type and 745 c-type RR Lyrae, selected using classifications and the *gi* color index from Palaversa et al. (2013). The LINEAR light curves, completed with IDs, equatorial coordinates, and other data, were accessed using the astroML Python module.

2.2. ZTF Dataset

The Zwicky Transient Facility (ZTF) is an optical time-domain survey that uses the Palomar 48-inch Schmidt telescope and a camera with 47 deg^2 field of view (Bellm et al. 2019). The data analyzed here was obtained with SDSS-like *g*, *r*, and *i* band filters. Light curves for objects in common with the LINEAR RR Lyrae sample typically have smaller random photometric errors than LINEAR light curves because ZTF data are deeper (compared to LINEAR, ZTF data have about 2-3 magnitudes fainter 5σ depth).

The ZTF dataset for this project was created by selecting ZTF IDs with matching equatorial coordinates to a corresponding LINEAR ID of an RR Lyrae star. This process used the *ztfquery* function, which searched the coordinates database within a r~3. Our sample consisted of 2857 stars.

2.3. Analysis of RR Lyrae stars

We used several methods and tools to analyze our RR Lyrae star sample thoroughly. Previous research has shown that the Blazhko effect presents itself as a modulation of period or amplitude, or it is visible in the star's periodogram. In the following section, we describe methods for such analysis.

The periodic shape change of light curves for Blazhko stars is equivalent to periodic phase and amplitude changes of the harmonics that make up the light curve. This work used the Lomb-Scargle method for period calculation and periodogram analysis. By finding specific harmonics that create the final shape of the light curve and representing their power of fit using a periodogram, we can find a potential *blazhko frequency*.

Comparing the Blazhko effect as a *blazhko frequency* interfering with the intrinsic frequency of pulsation of an RR Lyrae, it is observed that modulation of either period or amplitude arises. The effect is known as **interference beats**, described by the equation below:

$$y(t) = 2\,cos(2\pi\,\Delta f)\,sin(2\pi\,f_{avg}) \quad (1)$$

Where Δf is the difference between the primary and Blazhko frequency, and f_{avg} is the average between the two frequencies.

A periodogram from a Blazhko star would contain a central peak with two equally distant local peaks at frequencies f_- and f_+, with $f_- < f_0 < f_+$, where f_0 is the frequency of the main pulsation. The sideband peaks can be highly asymmetric Alcock et al. (2003). Observing periodograms can sometimes be much more complex Szczygieł & Fabrycky (2007).

For this project, we created an algorithm that searches for an interfering *blazhko frequency* by folding the periodogram through the main peak and comparing if the folded peaks were statistically more significant than the background noise. The algorithm utilized the increased SNR due to the multiplication of peaks. It also eliminated stars with a yearly alias.

The Blazhko period, calculated if the algorithm finds the Blazhko frequency, is defined as

$$P_{BL} = |f_{-,+} - f_0|^{-1}, \quad (2)$$

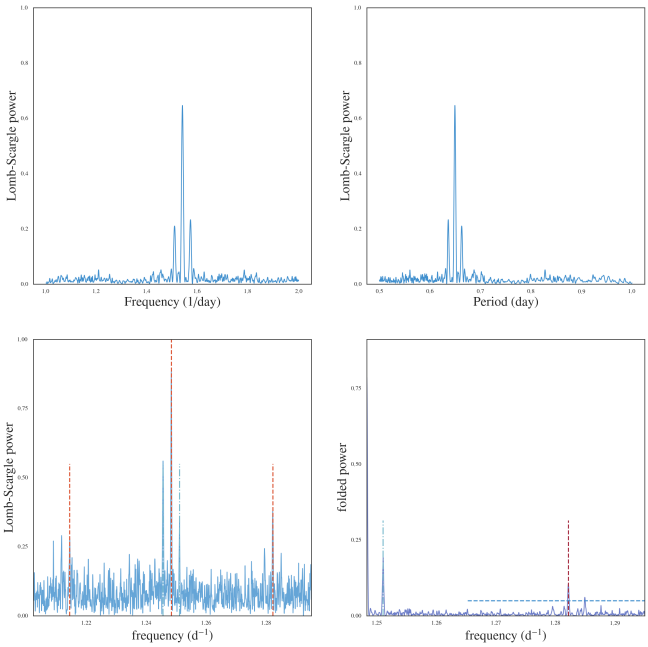

Fig. 1. Comparison of theoretical interference beats for a simulated light curve and real periodogram data from LINEAR and ZTF datasets.

where $f_{-,+}$ means the Blazhko sideband frequency with a higher amplitude is chosen.

The observed Blazhko periods range from 3 to 3,000 days, and Blazhko amplitudes range from 0.01 mag to about 0.3 mag (Szczygieł & Fabrycky 2007). In this work, we select a smaller Blazhko range due to the range of our data.

Fig 1 compares the theoretical periodogram produced by interference beats with our algorithm's periodogram, signifying that local Blazhko peaks are present in real data.

The Blazhko effect most commonly presents as a modulation of amplitude, period, or both. We phased the light curves, calculated their fit, and χ^2 value was also calculated. The χ^2 value gives a quantitative representation of *"goodness of fit"*, which shows us if modulation is present. Fig 2 shows an example star with LINEAR and ZTF phased light curves, along with their *fits*.

2.4. Searching for the Blazhko Effect

For efficient and robust analysis, another algorithm was developed to select viable Blazhko candidates to be visually analyzed. The algorithm removed all stars with unrealistic data or insufficient data points (250 for LINEAR and 40 for ZTF). Then, it removed stars whose *blazhko peak* was a yearly/daily alias, whose relative strength of peaks was below 0.05, and whose significance was below 5—their Blazhko period had to be between 30 and 325 days. The selection of stars based on the period difference (difference between LINEAR and ZTF period, divided by the mean period), amplitude, and the χ^2 value was made using a scoring mechanism. Based on the distribution of period differences and χ^2 values, it was determined for LINEAR that $1.8 < \chi^2 < 3.0$ was worth 2 and $\chi^2 > 3.0$ worth 3 points, while for ZTF $2.0 < \chi^2 < 4.0$ and $\chi^2 > 4.0$ were the limits. If both χ^2 parameters were satisfied, it was worth 4 or 6 points, respective of the limits. The limits of the period difference were $0.00002 < dP < 0.00005$ worth 2, and $dP > 0.00005$ worth 4 points. Finally, $0.05 < ample < 0.15$ was worth one, and

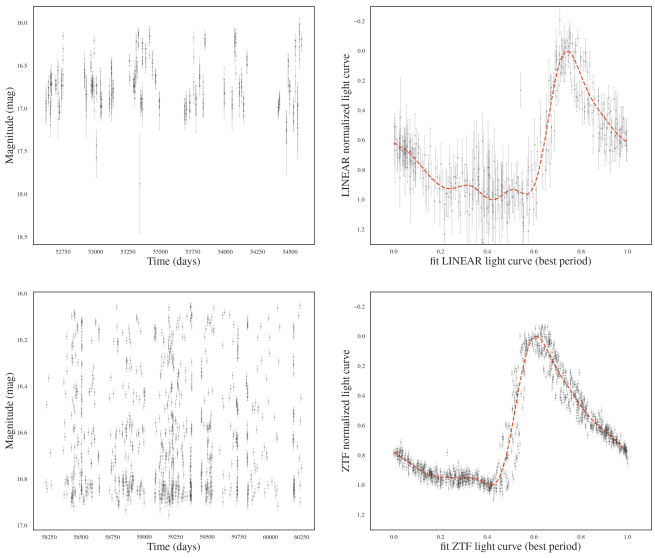

Fig. 2. Comparison of theoretical interference beats for a simulated light curve and real periodogram data from LINEAR and ZTF datasets.

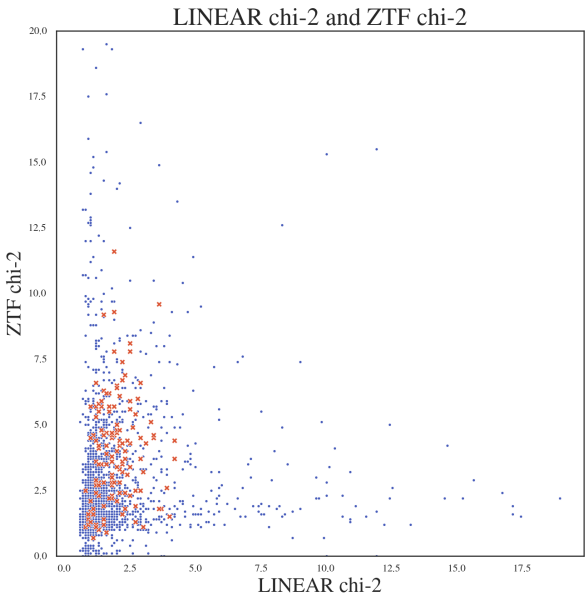

Fig. 3. χ^2 values for LINEAR and ZTF, where blue are all RR Lyrae stars and red are Blazhko stars.

$0.15 < ample < 2.00$ was worth 2 points. A star could score a maximum of 12 points or be directly selected via its *blazhko frequency*. A smaller sample of 239 Blazhko candidates was selected. Visual analysis was separated into five categories: LINEAR or ZTF *blazhko frequency*, LINEAR or ZTF χ^2 value, and none of the above.

Firstly, the shape and noisiness of the phased light curves were examined. If it was deemed that the light curve was precise enough, and if the phase contained different shapes. Fig 4 shows the first phase of visual analysis, where the ZTF fit shows signs of the Blazhko effect.

Secondly, the correctness of the algorithm in recognizing the *blazhko frequency* was examined. Fig 5 shows an example where the LINEAR periodogram is a perfect example of how the algorithm correctly identifies two very prominent peaks. If the peaks were aligned with the yearly aliases (like for the ZTF counterpart) or were not statistically significant, or if the algorithm detected a false signal, the star did not satisfy this phase.

Thirdly, the general shape of the light curve was examined. Fig 6 depicts a case where the criteria are not satisfied: the overall shape of the data is rectangular, with perhaps slight amplitude modulation, which is unnoticeable. The criteria would be satisfied if the data had a clear wave-like pattern.

The final phase is the most important, analyzing the light curve fit for each observation season. Fig 7 shows an example of a Blazhko star, where from season to season, we can notice slight **phase and amplitude modulation** in the LINEAR data, while in the ZTF data, the phase modulation is quite visible.

If a star has satisfied the criteria of the first and final stage, only the second stage, or all four stages, it is most likely a Blazhko star. After visually analyzing the starting 239 Blazhko candidates, only 136 remain confirmed Blazhko stars.

3. Results

After analysis of 2857 RR Lyrae stars from LINEAR and ZTF data, we found 136 Blazhko field stars. In Appendix A, the reader can find all of the Blazhko stars and some elementary data describing each star.

In the Blazhko star sample, most were selected by a high χ^2 value in the ZTF dataset rather than in the LINEAR dataset, as shown in the following figure.

Another important note highlighting the difficulty of finding Blazhko stars is that the absolute Blazhko frequency difference from the main frequency is approximately 0.028 d^{-1}. Also, the average period difference between LINEAR and ZTF in Blazhko stars was around 0.0001 days. These minimal differences require precise observations over a long temporal baseline. The distribution of RRab and RRc type RR Lyrae in our sample is representative of other surveys, where 71% were type RRab and 29% RRc type.

Finally, we have discovered that in some Blazhko stars, the effect cannot be detected ten years later or beforehand. When comparing LINEAR and ZTF data, some pairs have the effect present in only one dataset and others in both. This finding could mean that the Blazhko effect is not always present and gives us a clue about its mechanism. However, the precision of data is also a factor for consideration.

4. Discussion and Conclusions

The reported incidence rates for the Blazhko effect range from 5% (Szczygieł & Fabrycky 2007) to 60% (Szabó et al. 2014). For a relatively small sample of 151 stars with Kepler data, a claim has been made that essentially every RR Lyrae star exhibits modulated light curve (Kovacs 2018). The difference in Blazhko incidence rates for the two most extensive samples, obtained by the OGLE-III survey for the Large Magellanic Cloud (LMC, 20% out of 17,693 stars; Soszyński et al. 2009). Moreover, the Galactic bulge (30% out of 11,756 stars; Soszyński et al. 2011) indicates a possible variation of the Blazhko incidence rate with underlying stellar population properties. In this work, 4.67% of the original RR Lyrae dataset are Blazhko stars. Since our sample size is considerable, we conclude that the incidence rate of Blazhko stars in our work is representative and aligns with other

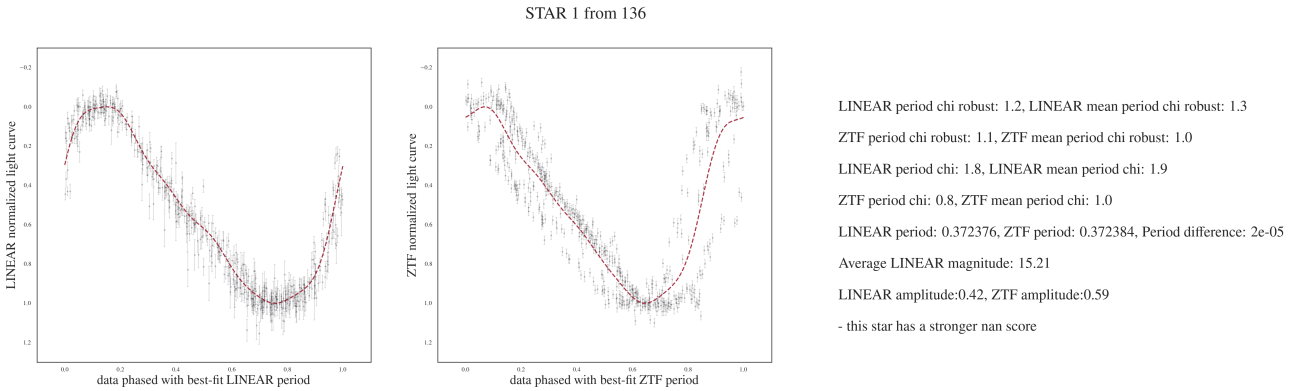

Fig. 4. Phase 1 of visual analysis of Blazhko candidates.

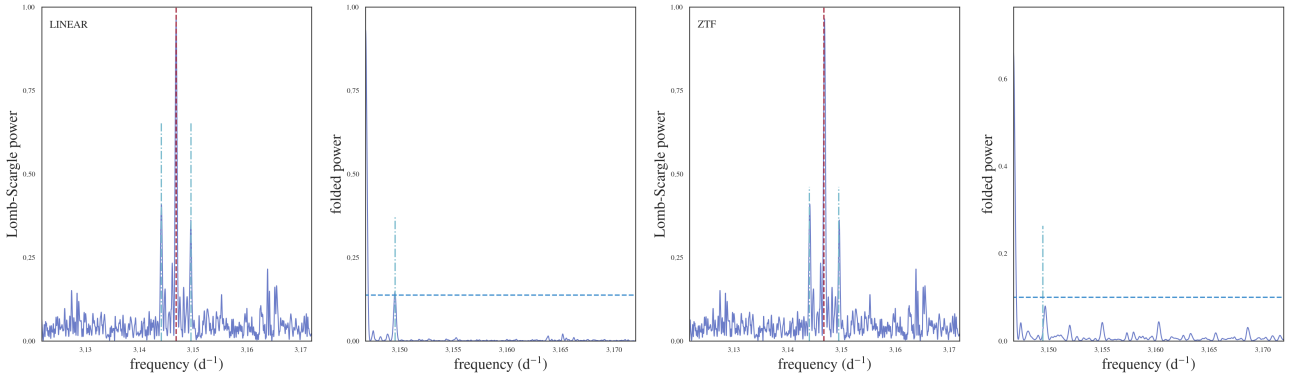

Fig. 5. Phase 2 of visual analysis of Blazhko candidates.

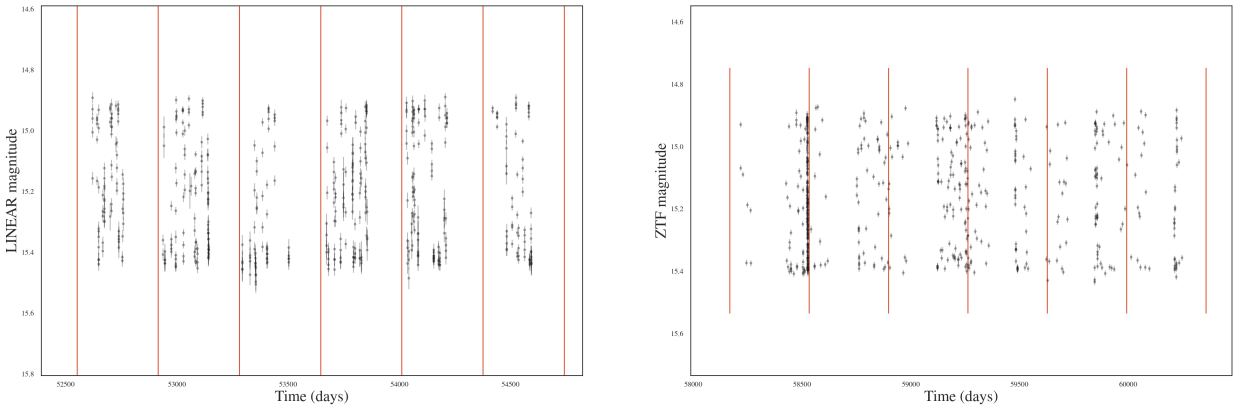

Fig. 6. Phase 3 of visual analysis of Blazhko candidates.

works. We theorize that the difference in incidence rates occurs due to varying data precision, the temporal baseline length, and differences in visual or algorithmic analysis. We also conclude that our algorithm's success rate in finding 136 out of 239 potential Blazhko stars is 57% . This high number indicates that the algorithm is very successful and can be used and refined further for efficient Blazhko star selection.

For future research, we would like to explore the final finding and find a connection or a factor that might give rise to a mechanism that explains the Blazhko effect. The project is an excellent example of automatizing the search for Blazhko stars. It can further be improved by training a neural network to replace visual analysis, and our current algorithms can be improved with other models. This work can provide a base for finding more Blazhko stars for the future Vera Rubin observatory. The Legacy Survey of Space and Time (LSST; Ivezić et al. 2019) will be an excellent survey for studying Blazhko effect (Hernitschek & Stassun 2022) because it will have both a long temporal baseline (10 years) and a large number of observations per object (nominally 825; LSST Science Requirements Document[2]). We hope this work helped in the ongoing research on the Blazhko effect.

Acknowledgements. LINEAR and ZTF acknowledgements. Thanks to Mathew Graham for *ztfquery* example. Ž.I. acknowledges funding by the Fulbright Foundation and thanks the Ruđer Bošković Institute for hospitality.

[2] Available as ls.st/srd

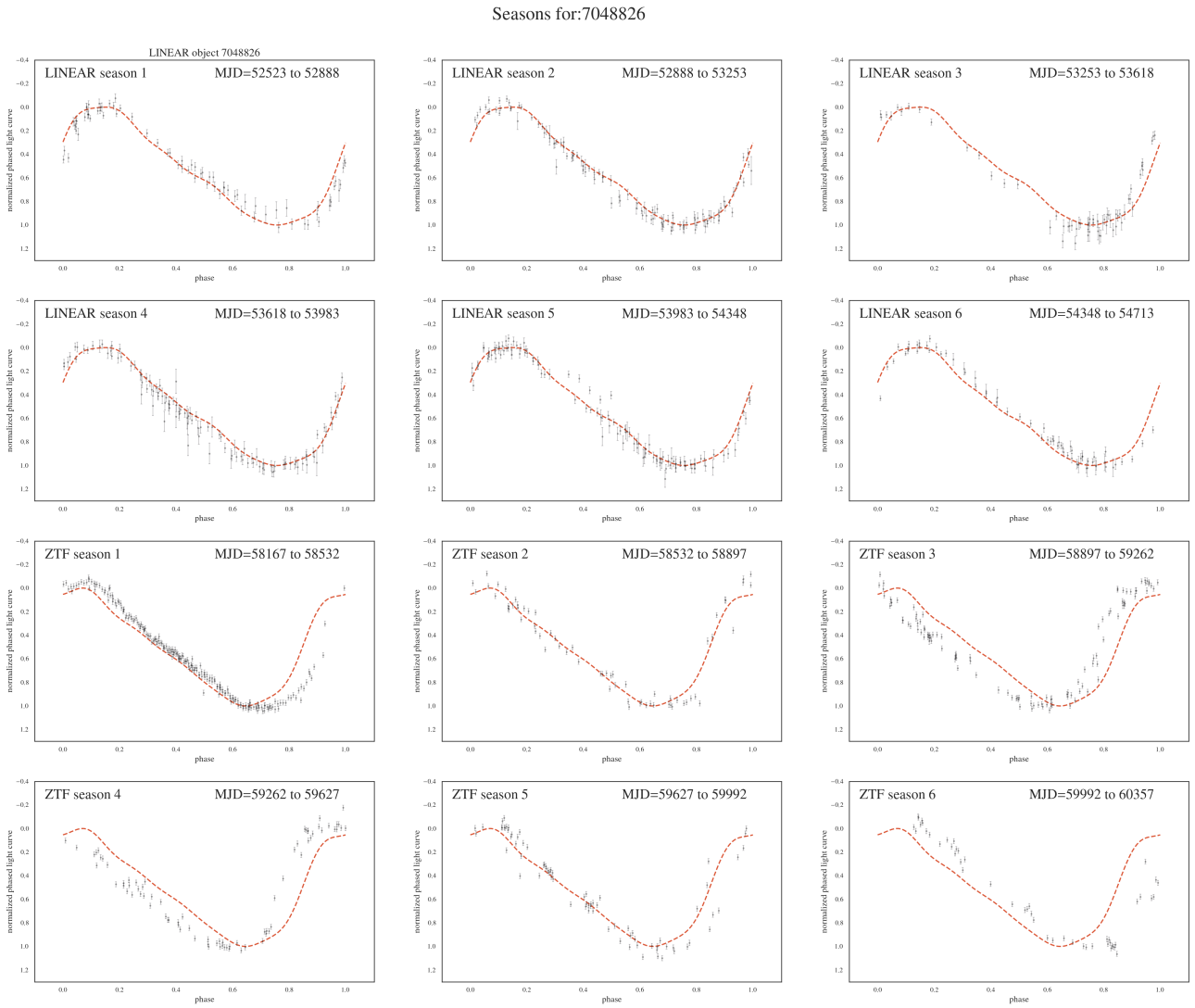

Fig. 7. Phase 4 of visual analysis of Blazhko candidates.

References

Alcock, C., Alves, D. R., Becker, A., et al. 2003, ApJ, 598, 597
Bellm, E. C., Kulkarni, S. R., Graham, M. J., et al. 2019, PASP, 131, 018002
Benkő, J. M., Kolenberg, K., Szabó, R., et al. 2010, MNRAS, 409, 1585
Blažko, S. 1907, Astronomische Nachrichten, 175, 325
Catelan, M. 2009, Ap&SS, 320, 261
Hernitschek, N. & Stassun, K. G. 2022, ApJS, 258, 4
Ivezić, Ž., Kahn, S. M., Tyson, J. A., et al. 2019, ApJ, 873, 111
Kovács, G. 2009, in American Institute of Physics Conference Series, Vol. 1170, Stellar Pulsation: Challenges for Theory and Observation, ed. J. A. Guzik & P. A. Bradley, 261–272
Kovacs, G. 2016, Commmunications of the Konkoly Observatory Hungary, 105, 61
Kovacs, G. 2018, A&A, 614, L4
Mizerski, T. 2003, Acta Astron., 53, 307
Palaversa, L., Ivezić, Ž., Eyer, L., et al. 2013, AJ, 146, 101
Sesar, B., Ivezić, Ž., Grammer, S. H., et al. 2010, ApJ, 708, 717
Sesar, B., Ivezić, Ž., Stuart, J. S., et al. 2013, AJ, 146, 21
Sesar, B., Stuart, J. S., Ivezić, Ž., et al. 2011, AJ, 142, 190
Smith, H. A. 1995, Cambridge Astrophysics Series, 27
Soszyński, I., Dziembowski, W. A., Udalski, A., et al. 2011, Acta Astron., 61, 1
Soszyński, I., Udalski, A., Szymański, M. K., et al. 2010, Acta Astron., 60, 165
Soszyński, I., Udalski, A., Szymański, M. K., et al. 2009, Acta Astron., 59, 1
Szabó, R., Benkő, J. M., Paparó, M., et al. 2014, A&A, 570, A100
Szczygieł, D. M. & Fabrycky, D. C. 2007, MNRAS, 377, 1263

Appendix A: Full table of results

Here we present all the confirmed Blazhko stars with their LINEAR IDs, equatorial coordinates, and calculated periods and χ^2 values.

LINEAR ID	RA	DEC	LINEAR period	ZTF period	LINEAR chi-2	ZTF chi-2
523832	207.529404	33.706001	0.372376	0.372384	1.20	1.10
1240665	206.202469	34.058662	0.632528	0.632522	3.00	1.10
1736308	206.096115	36.648674	0.555848	0.555843	1.30	1.00
2669011	206.229523	38.758453	0.591153	0.591151	1.10	0.70
2742032	207.355225	39.589951	0.629676	0.629692	0.90	1.40
2812086	206.805511	40.859066	0.646015	0.646000	3.00	3.20
3507643	206.557358	39.536449	0.801141	0.801132	1.60	0.90
5931160	207.177231	41.918797	0.664700	0.664708	0.80	1.10
6665721	206.020233	41.646141	0.643318	0.643325	1.00	1.70
17185566	206.387268	43.314617	0.614160	0.614169	1.50	1.90
22828215	206.657028	43.543236	0.574536	0.574535	1.50	1.40
29848	206.917358	44.971054	0.557020	0.557040	1.40	3.50
158779	207.772202	45.916824	0.609207	0.609189	1.60	3.90
263541	207.172470	45.713154	0.558218	0.558221	2.90	6.60
514883	206.594757	46.482040	0.557723	0.557737	1.70	5.50
737951	206.435547	45.881615	0.357023	0.357023	2.20	6.70
810169	169.297485	6.265203	0.465185	0.465212	2.10	2.80
924301	169.713531	6.963072	0.507503	0.507440	1.90	9.30
1092244	207.060974	5.649392	0.649496	0.649558	1.20	3.60
1244554	206.944962	5.346962	0.536875	0.536962	1.80	2.30
1307948	206.223587	6.741248	0.527474	0.527415	1.80	4.50
1332201	207.992432	-4.603579	0.580711	0.580731	1.60	4.20
1390653	207.220245	-3.214271	0.521867	0.521871	1.30	4.10
1435279	207.824600	-3.712567	0.381858	0.381860	2.10	4.20
1448299	206.582916	51.406654	0.606912	0.606940	2.70	5.40
1593736	169.096771	5.428976	0.592628	0.592650	1.20	5.70
1748058	207.353790	53.020401	0.310237	0.310176	1.40	5.70
1857382	206.026001	56.421604	0.566428	0.566407	2.70	2.50
1882354	207.117645	56.313797	0.695061	0.695029	1.50	2.80
2041979	206.848053	55.248009	0.653694	0.653639	1.20	5.30
2075949	207.733643	62.320267	0.477806	0.477666	1.60	4.70
2117028	207.188278	61.978554	0.591245	0.591243	2.20	3.50
2122319	206.210190	62.778843	0.359422	0.359424	2.10	6.10
2229607	207.042603	65.877083	0.575179	0.575211	1.20	4.40
2243683	206.780823	8.893113	0.579777	0.579803	3.10	4.30
2248787	206.407776	7.914382	0.563528	0.563539	2.10	2.40
2334384	206.454544	7.380644	0.555341	0.555333	2.00	6.50
2397296	168.680649	51.998081	0.488814	0.488836	1.20	6.60
2414841	206.101624	7.666218	0.559611	0.559592	1.70	5.70
2455568	168.211075	51.534416	0.594119	0.594092	2.00	2.10
2612592	207.693237	-5.975360	0.571562	0.571543	1.30	2.80
2653982	168.135025	51.014339	0.607082	0.607110	1.00	2.10
2766997	207.782440	-7.099904	0.289881	0.289943	1.80	3.60
2892940	209.495773	2.587467	0.539855	0.539896	1.30	4.20
3036295	209.338211	2.393512	0.629705	0.629714	1.80	2.20
3140139	208.758163	-0.100046	0.304590	0.304585	2.50	5.60
3183285	208.391159	0.479103	0.349653	0.349664	1.20	2.80
3196582	208.521881	0.740297	0.268017	0.268018	2.50	3.40
3196780	169.384384	53.303658	0.504148	0.504199	2.20	3.20
3294319	169.550766	53.459976	0.555460	0.555473	1.90	4.70
3437725	208.845749	12.514306	0.542457	0.542478	1.50	6.30
3591037	208.146072	14.167974	0.558643	0.558609	1.30	3.50
3941776	209.073120	13.401526	0.532222	0.532209	2.80	6.00
4101289	209.351425	13.537904	0.379225	0.379250	1.20	2.70
4586691	208.326218	15.475822	0.621459	0.621446	2.00	3.40
4804945	209.674210	16.421736	0.556172	0.556217	2.50	7.80
5421989	208.014435	18.561077	0.534510	0.534527	0.80	2.50

LINEAR ID	RA	DEC	LINEAR period	ZTF period	LINEAR chi-2	ZTF chi-2
6582265	209.421219	17.441139	0.691751	0.691749	2.90	3.70
6651516	208.909760	17.881287	0.308488	0.308496	1.30	5.80
6819457	209.491974	20.296762	0.436282	0.436265	3.60	9.60
6883239	208.333481	19.276327	0.563711	0.563712	2.90	2.50
6967017	208.406662	21.846382	0.529691	0.529677	2.30	6.90
7048826	208.492981	22.591896	0.317781	0.317790	1.40	5.90
7254801	209.648148	22.561989	0.561133	0.561071	1.30	5.50
7279621	208.915436	24.833937	0.415469	0.415467	1.90	4.60
7283275	208.409698	26.350325	0.543342	0.543331	2.20	3.60
7344401	209.188583	26.111385	0.330201	0.330226	1.80	2.70
7580734	209.349243	26.322409	0.314956	0.314957	2.00	4.00
7657340	208.098282	27.700201	0.495480	0.495493	2.30	4.00
7811366	208.457687	30.868412	0.489523	0.489521	2.00	4.70
7827663	208.047531	30.799057	0.390832	0.390832	3.40	4.50
7846640	209.106400	4.330462	0.551495	0.551518	1.50	9.20
8222011	209.258850	3.100914	0.350920	0.350914	2.00	4.80
8311517	208.212936	4.452833	0.523354	0.523359	1.80	3.60
8331094	208.446945	3.969552	0.267543	0.267549	2.10	3.30
8343291	208.919601	-2.689821	0.569785	0.569791	3.30	5.10
9063194	169.357468	57.331566	0.575781	0.575760	2.40	3.10
9236215	209.009872	-1.607280	0.352570	0.352572	1.80	2.80
9449335	209.488937	-2.928472	0.475720	0.475695	2.00	5.00
9532981	168.695602	60.104759	0.591000	0.591042	1.70	6.20
9918809	209.255295	-2.089725	0.479460	0.479509	1.90	11.60
9968431	209.717804	-2.437493	0.302266	0.302211	1.70	2.20
9979905	208.905365	31.572962	0.338739	0.338739	2.50	2.30
10030349	209.547668	32.537975	0.545073	0.545074	2.10	4.40
10260828	208.891602	32.249817	0.380655	0.380643	2.20	7.40
10814742	209.570526	31.039347	0.462687	0.462683	2.50	4.30
11215595	208.180191	33.574619	0.546960	0.546943	1.30	2.30
16991760	209.105652	33.977589	0.549098	0.549096	2.90	3.70
17247918	169.489120	59.391106	0.481867	0.481865	1.80	4.60
17275627	208.806717	33.957424	0.537775	0.537771	2.10	4.80
17302403	209.807205	35.285717	0.488261	0.488343	2.00	6.40
17544856	208.748581	36.859768	0.614297	0.614296	2.00	3.40
19775800	208.958618	36.484657	0.310856	0.310867	1.30	2.70
21488669	209.334930	37.248749	0.501644	0.501661	1.90	5.70
21556651	208.269577	38.000725	0.614826	0.614808	1.80	3.10
21619184	208.125366	37.095997	0.557343	0.557320	2.30	3.70
21806402	208.151657	39.543987	0.592081	0.592104	1.60	6.20
21874209	209.602371	40.245346	0.611295	0.611286	2.50	5.90
21967825	209.202347	39.452202	0.540607	0.540600	1.80	4.70
22244513	208.742203	41.386112	0.604149	0.604077	2.50	8.10
22319996	209.734711	42.773571	0.479505	0.479495	2.60	4.90
22518636	208.239105	41.299026	0.283996	0.283998	1.80	3.00
22959674	209.018127	41.835575	0.405333	0.405409	1.80	3.80
22980793	208.105713	44.400867	0.540348	0.540353	1.90	2.80
23135759	209.604721	45.746510	0.402730	0.402732	4.20	4.40
23148883	209.446594	45.757584	0.390130	0.390124	1.40	4.80
23184808	208.547745	47.825001	0.338821	0.338888	1.00	5.70
23193507	208.703445	49.226929	0.473158	0.473174	3.40	4.60
23653629	209.116013	50.653641	0.442052	0.442055	2.40	4.40
24019356	208.649506	50.454273	0.517473	0.517460	1.50	4.60
24020106	209.853088	5.836339	0.542397	0.542396	2.90	4.50
24216004	209.385406	6.251467	0.382077	0.381912	1.90	7.80
880588	208.532242	6.762656	0.600138	0.600134	1.20	2.40
1212611	208.592422	6.144436	0.630896	0.630893	0.90	1.20
1876491	209.131027	5.983884	0.760128	0.760123	1.20	1.20
3048546	209.125137	-4.194337	0.656287	0.656293	1.00	1.30
5272753	208.115189	-4.847239	0.485827	0.485831	0.90	1.60
8610884	208.744736	-4.852155	0.592421	0.592429	2.20	4.30
8907563	209.521454	-3.322183	0.513164	0.513164	1.10	4.60

LINEAR ID	RA	DEC	LINEAR period	ZTF period	LINEAR chi-2	ZTF chi-2
9852554	208.390961	-4.619442	0.651339	0.651367	1.00	4.50
9961135	209.178848	52.903030	0.590896	0.590891	1.10	1.80
10503746	208.417831	54.266953	0.573563	0.573570	2.70	1.90
21948290	209.862518	56.455978	0.511127	0.511115	2.30	2.40
23596342	209.988663	56.828396	0.602841	0.602846	1.20	2.90
23898397	121.150764	42.483574	0.563018	0.562989	1.60	3.50
1882088	208.323578	58.245502	0.315984	0.316041	4.00	1.50
2936953	208.351578	57.226521	0.328746	0.328733	2.70	1.30
3219035	209.858856	60.601982	0.326746	0.326509	3.90	2.60
4320492	168.062149	65.801857	0.361005	0.360942	3.70	1.80
8036191	208.732498	59.448402	0.363860	0.363893	2.20	1.60
10420063	209.945786	61.264187	0.487395	0.487394	4.20	3.70
10662468	209.124405	61.076996	0.445180	0.445167	3.60	1.80
21688272	209.311371	62.800976	0.304803	0.304790	2.30	1.80
2714034	168.354202	65.678604	0.610868	0.610800	1.50	1.20
5592590	208.440872	65.857277	0.346945	0.346980	1.20	1.10
8799313	208.821136	7.846983	0.327560	0.327542	1.10	1.60